

Identifying Robust Decarbonization	001
Pathways for the Western U.S. Electric Power	002
System under Deep Climate Uncertainty	003
	004
	005
	006
	007
	008
	009
	010
	011
	012
Srihari Sundar ¹ , Flavio Lehner ^{2,3,4} , Nathalie Voisin ^{5,6}	013
and Michael T. Craig ^{7,8*}	014
	015
¹ Department of Aerospace Engineering, University of Michigan,	016
Ann Arbor, Michigan, USA.	017
² Department of Earth and Atmospheric Sciences, Cornell	018
University, Ithaca, NY, USA.	019
³ Climate and Global Dynamics Laboratory, National Center for	020
Atmospheric Research, Boulder, CO, USA.	021
⁴ Polar Bears International, Bozeman, MT, USA.	022
⁵ Pacific Northwest National Laboratory, Richland, WA, USA.	023
⁶ University of Washington, Seattle, WA, USA.	024
⁷ School for Environment and Sustainability, University of	025
Michigan, Ann Arbor, Michigan, USA.	026
⁸ Department of Industrial and Operations Engineering,	027
University of Michigan, Ann Arbor, Michigan, USA.	028
	029
	030
	031
*Corresponding author(s). E-mail(s): mtcraig@umich.edu ;	032
	033
	034
Abstract	035
Climate change threatens the resource adequacy of future power systems.	036
Existing research and practice lack frameworks for identifying decarbonization pathways that are robust to climate-related uncertainty. We	037
create such an analytical framework, then use it to assess the robustness	038
of alternative pathways to achieving 60% emissions reductions from 2022	039
levels by 2040 for the Western U.S. power system. Our framework integrates	040
power system planning and resource adequacy models with 100	041
climate realizations from a large climate ensemble. Climate realizations	042
drive electricity demand; thermal plant availability; and wind, solar, and	043
hydropower generation. Among five initial decarbonization pathways, all	044
exhibit modest to significant resource adequacy failures under climate	045
	046

2 *RDM decarbonization*

047 realizations in 2040, but certain pathways experience significantly less
048 resource adequacy failures at little additional cost relative to other pathways.
049 By identifying and planning for an extreme climate realization that
050 drives the largest resource adequacy failures across our pathways, we
051 produce a new decarbonization pathway that has no resource adequacy
052 failures under any climate realizations. This new pathway is roughly 5%
053 more expensive than other pathways due to greater capacity investment,
054 and shifts investment from wind to solar and natural gas generators.
055 Our analysis suggests modest increases in investment costs can add
056 significant robustness against climate change in decarbonizing power sys-
057 tems. Our framework can help power system planners adapt to climate
058 change by stress testing future plans to potential climate realizations,
059 and offers a unique bridge between energy system and climate modelling.
060

061 **Keywords:** robust decision-making, climate adaptation, capacity expansion,
062 single model initial condition large ensemble, power system decarbonization
063

064

1 Introduction

065 Rapidly transitioning to a decarbonized electric power sector is crucial to
066 aggressively mitigate climate change and meet emissions reductions targets
067 [1, 2]. In the United States, the Inflation Reduction Act (IRA) is poised to
068 accelerate low-carbon investments in the power sector, which could approach
069 370 billion USD by 2033 [3, 4]. Which power sector decarbonization pathway
070 will be taken remains uncertain, where a pathway is defined by where, when,
071 and what decarbonization investments occur [5–11]. As they decarbonize, bulk
072 (or transmission-scale) power systems will be increasingly affected by climate
073 change [12]. Increasing ambient air temperatures will increase peak and total
074 electricity demand [13–15] and reduce available capacity from thermal and
075 solar generators [13, 16–18]. Wind, solar, and precipitation changes will also
076 affect wind, solar, and hydropower generation potential [13, 19–21]. These
077 effects could compound to undermine resource adequacy (RA), or a system’s
078 ability to continually balance electricity supply and demand [22–24]. Under-
079 standing the vulnerability of decarbonizing power systems to potential future
080 climate realizations is critical for achieving reliable, affordable, and clean power
081 systems - the focus of our study [9, 25].
082

083 To account for decarbonization- and climate-related uncertainty in invest-
084 ment decisions, prior literature optimizes capacity investment decisions given
085 different decarbonization pathways and future climate scenarios [5, 9, 26–32].
086 This literature uses sensitivity or scenario analysis to incorporate climate-
087 related uncertainty within deterministic modeling frameworks. For instance,
088 Fonseca et al. [5] sample 3 of 20 global climate models (GCMs) to include
089 as scenarios in a deterministic long-term power system planning model. In
090 other words, this literature aims to improve investment decisions by improv-
091 ing predictions of future weather within standard modeling frameworks -
092

a "predict-then-act" approach to climate adaptation. But climate change poses deep uncertainty [33], which undermines the value of "predict-then-act" approaches [34], particularly for power system planning models that must significantly simplify uncertainty to remain computationally tractable. Deep uncertainty is characterized by uncertainty in how a system works and its boundaries, which leads to significant uncertainty in the probability distributions of scenarios and consequences [34]. In the context of climate change, deep uncertainty arises from disagreement around which future CO_2 emissions pathway the globe will follow (i.e., emissions scenario uncertainty); global climatic changes resulting from those pathways (i.e., climate sensitivity and structural uncertainty); and local meteorological changes resulting from global climatic changes (i.e., parametric uncertainty) [35–37]. In the near-term (prior to 2050), inter-annual (or internal) climate variability, which is driven by the dynamics of the climate system and sensitive to initial conditions [38–41], is the primary source of climate-related uncertainty [40, 42]. Under deep uncertainty, methods focused on identifying robust strategies or alternatives are better suited to informing decisions than "predict-then-act" methods [34]. Such decision support is urgently needed by power system planners and regulators, who are tasked with ensuring resource adequacy across a wide range of potential future climate realizations, which combine secular trends and inter-annual climate variability [41]. Recent rolling outages in California and Texas [43, 44] and resource adequacy warnings elsewhere in the United States [45] underscore this urgency.

In response to these needs, we construct a new analytical framework for planning decarbonizing power systems under deep climate uncertainty by drawing on a concept from the decision science literature: robust decision making (RDM) [34, 46]. RDM has been used to inform climate adaptation strategies, e.g. in water resources management [47–53]. It has also been used in the power sector, e.g. to evaluate policy strategies for European power systems against shocks [54]. But our framework is the first to apply RDM to planning decarbonizing power systems under deep climate uncertainty. By integrating power system planning and operational models with potential climate realizations from a single model initial-condition large ensemble (SMILE) [55, 56], our framework generates alternative decarbonization pathways; characterizes the vulnerability of and trade-offs between those pathways under potential climate realizations; and uses generated insights to identify new alternative decarbonization pathways that are robust to climate-related uncertainty (Figure 1). SMILEs have limited prior use in power systems research [57, 58] even though they are designed to sample inter-annual variability and provide many realizations of future climate, encoding multiple extreme events and a range of possible meteorological projections [59, 60].

We use our framework to answer: how can we design decarbonizing power systems to be robust against deep climate uncertainty? We conduct our study for the U.S. Western Interconnect, which we divide into five subregions per Western Electricity Coordinating Council's resource adequacy assessments

4 *RDM decarbonization*

139 (Figure E.1, [61]). We use 100 members from the Community Earth System
140 Model 2 (CESM2) Large Ensemble (LENS2) through 2040, which was driven
141 by the SSP3-7.0 emissions scenario and reaches 1.65°C of global warming by
142 2040 relative to pre-industrial [62]. For each ensemble member, we obtain sur-
143 face air temperatures, relative humidity, surface solar radiation, 10m wind
144 speeds, and total runoff at daily and 1° spatial resolution (approx. 100 km by
145 100 km) through 2040 across our study region. While this resolution is lower
146 than what is preferred for power system modeling, higher resolution climate
147 datasets often do not sample as large of a range of internal climate variability
148 as LENS2, particularly in the time-span of interest to us (through 2040) and
149 when focused on extreme events. In selecting LENS2, we also emphasize inter-
150 internal variability over climate response uncertainty. For each ensemble member,
151 we translate meteorological variables to spatially-explicit timeseries of elec-
152 tricity demand; maximum potential wind, solar, and hydropower generation;
153 and thermal generator deratings and forced outage rates. To analyze the vul-
154 nerability and trade-offs of alternative decarbonization pathways, we generate
155 five decarbonization pathways by running a capacity expansion (or long-term
156 planning) model of the Western Interconnect using power system variables
157 from five sampled ensemble members. Our decarbonization pathways reduce
158 interconnect-wide power system CO₂ emissions by 60% from 2022 levels by
159 2040. For each decarbonization pathway, we approximate its regional resource
160 adequacy in 2040 under each of the 100 ensemble members using economic
161 dispatch and surplus available capacity models. From this large set of alter-
162 native future systems and climate realizations, we examine vulnerabilities and
163 trade-offs of these decarbonization pathways across potential climate realiza-
164 tions. Finally, we identify a future climate realization that generates the largest
165 resource adequacy failures across decarbonization pathways in 2040, then use
166 that climate realization to generate a new decarbonization pathway robust to
167 all 100 ensemble members.

168

169

170

171

172

173

174

175

176

177

178

179

180

181

182

183

184

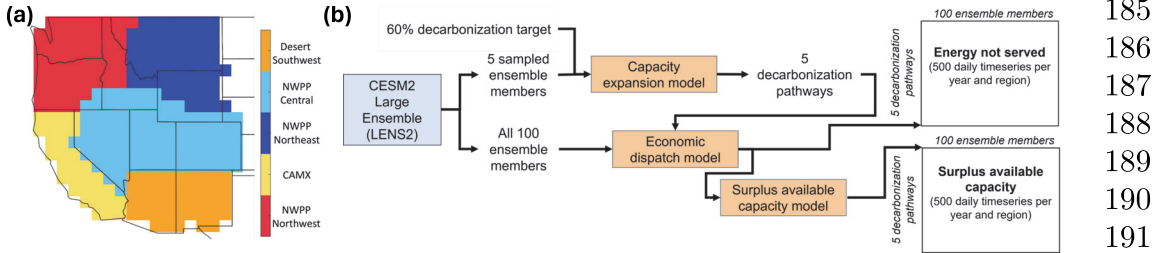


Fig. 1: (a) Map of our Western Interconnect study region, which is divided into 5 sub-regions (differentiated by color). Blocks at edges of interconnect correspond to LENS2 grid cells. CAMX stands for California and Mexico and NWPP stands for Northwest Power Pool. (b) Our analytical framework integrates 100 ensemble members (or climate realizations) from the LENS2 dataset with power system capacity expansion, economic dispatch, and surplus available capacity (SAC) models. For each region, this framework yields 500 annual timeseries of daily energy not served and surplus available capacity in 2040, or 1 annual timeseries of daily values (or "daily timeseries") for each climate realization, decarbonization pathway, and metric. Not shown is identification of an extreme 2040 climate realization, which is then fed back into the capacity expansion model to generate a new decarbonization pathway.

2 Methods

2.1 Robust Decision-making Framework

We use robust decision-making (RDM) to quantify the robustness of alternative decarbonization pathways in the Western Interconnect power system to potential future climate realizations. We first conduct exploratory modeling to generate five decarbonization pathways for the Western Interconnect using a capacity expansion (or long-term planning) model (Section 2.2). We then stress test each decarbonization pathway to all 100 LENS2 ensemble members (Section 2.4). For each pathway and ensemble member, we approximate resource adequacy by quantifying daily Surplus Available Capacity (SAC) and Energy Not Served (ENS) in 2040 (Section 2.3). Finally, we identify the climate ensemble member that drives the largest combined energy not served (ENS) across decarbonization pathways in California (our largest load region) in 2040; rerun our planning model using that ensemble member; and quantify our resource adequacy metrics for that pathway against all 100 climate ensemble members.

The "XLRM" framework is a common starting point for RDM that frames the decision space available to stakeholders [34]. X indicates uncertainties outside decisionmaker control; L indicates policy levers, or near-term actions, available to decisionmakers; M indicates performance measures that can be used to compare future scenarios; and R indicates relationships between uncertainties (X) and levers (L) and how those relationships affect performance

185
186
187
188
189
190
191
192
193
194
195
196
197
198
199
200
201
202
203
204
205
206
207
208
209
210
211
212
213
214
215
216
217
218
219
220
221
222
223
224
225
226
227
228
229
230

231	X: Future climate realizations	L: Power system decarbonization pathways (composed of where, when, what type, and how much investment in generating and trans- mission occurs)
234	R: Response of power system assets to climate 235 change (including hydropower, thermal gener- 236 ators, wind power, solar power, and electricity 237 demand); capacity expansion model; resource 238 adequacy models	M: Daily and annual resource adequacy; Total 239 fixed plus variable system costs; Annual sys- 240 tem CO_2 emissions

Table 1: Our analysis represented within the XLRM framework

241 measures (M). Table 1 provides an XLRM framework for our analysis specif-
242 ically and for power system adaptation to climate change analyses more
243 generally.

244 **2.2 Capacity Expansion Model and Decarbonization 245 Pathways**

246 To generate alternative decarbonization pathways, we use a capacity expansion
247 (or long-term planning) model. We run the capacity expansion model (CEM)
248 in two year increments from 2023 to 2040, capturing coincident, spatially-
249 resolved meteorology and hydrology for each year (Section 2.4). The CEM
250 is a deterministic linear program that minimizes fixed plus variable costs by
251 deciding investment in wind plants, solar plants, and natural gas combined
252 cycle (NGCC) plants with or without carbon capture and sequestration (CCS),
253 and inter-regional transmission. These investment decisions differentiate our
254 “decarbonization pathways”. The CEM also optimizes operation of existing
255 and new generators, and optimizes inter-regional transmission flows using the
256 simplified transport method, which constrains inter-regional transmission flows
257 to a fixed power rating rather than modeling AC or DC power flow. The first
258 CEM run is initialized with the existing Western U.S. generator fleet and
259 inter-regional transmission capacity (SI.E). All generator capacity investment
260 decisions occur at the LEN52 grid cell level, i.e. on a 100 by 100 km grid across
261 our study region, while transmission investments occur at inter-regional levels.
262 We constrain thermal plant investments to grid cells that already contain large
263 thermal units. Given the immature state of CCS technology, we allow the
264 CEM to invest in NGCC or coal with CCS beginning in 2031. To capture
265 ongoing retirements of coal-fired power plants, we retire coal units with average
266 capacity factors of less than 0.3 after each CEM run [63]. While we recognize
267 the important role of grid-scale storage in decarbonizing power systems, our
268 climate data is only available at daily resolution (Section 2.4). As such, we
269 cannot model intra-day storage.

270 The CEM includes numerous system- and generator-level constraints.
271 At the system level, the CEM balances regional supply (generation plus
272 imports minus exports) and demand each day. We do not account for inter-
273 changes with Canada and Mexico. The CEM requires derated capacity to
274 exceed peak demand, where derated capacity accounts for wind and solar

generation potential; a fixed 5% forced outage rate for wind and solar generators; temperature-dependent FORs for thermal and hydropower plants; and weather-driven deratings of combustion turbine, combined cycle, and coal-fired plants. At the generator level, wind and solar generation is limited by daily, spatially-specific wind and solar capacity factors (Section 2.4); hydropower generation is constrained by subregional monthly total generation; and generation from combustion turbine, combined cycle, and coal-fired plants is limited by daily, spatially-specific meteorology. 277
278
279
280
281
282
283
284

With the CEM, we generate five decarbonization pathways that each reduce 285
interconnect-wide CO₂ emissions by 60% from 2022 levels by 2040. To 286
create these five pathways, we use meteorological timeseries from five sampled 287
LENS2 members. These ensemble members are sampled to capture a range of 288
warming and relative humidity changes within the LENS2 ensemble (Table 2). 289
Specifically, we quantify warming level based on the difference between his- 290
toric (1985-2015) and mid-century (2035-2065) mean surface temperature and 291
relative humidity [64]. Warming and relative humidity levels vary from 1.5 °C 292
to 2.75 °C and 0.1 to -1.79, respectively, across sampled ensemble members 293
(Figure B.1). We present results for each of these pathways by labeling them 294
from 1 to 5 (Table 2). In using five sampled ensemble members, our purpose 295
is to create heterogeneous decarbonization pathways that could all reach a 296
given decarbonization target, then assess the pathways' vulnerabilities, trade- 297
offs, and robustness. We do not create a pathway for each ensemble member 298
because creating pathways that span all climate- and decarbonization-related 299
uncertainty is not computationally tractable. Rather, researchers and practi- 300
tioners explore a subset of this uncertainty in analyses and long-term plans. 301
With respect to climate-related uncertainty, sampling algorithms are typically 302
used to identify a few weeks of one weather year for inclusion in planning 303
models. While these algorithms aim to capture periods that could threaten 304
system resource adequacy, they capture a limited range of potential climate 305
conditions, particularly when considering not just multiple weather years but 306
also multiple climate realizations. We therefore demonstrate our framework in 307
a similar context as is used in practice, i.e. on pathways that consider a sub- 308
set of relevant uncertainty. The CEM is programmed in the General Algebraic 309
Modeling System (GAMS) [65] and solved using CPLEX [66]. 310
311
312
313
314
315
316
317
318
319
320
321
322

Index	LENS2 Member ID	ΔT (°C)	ΔRH
1	r10i1191p1f2	2.50	-1.17
2	r5i1231p1f1	2.59	-1.79
3	r12i1301p1f2	1.70	0.10
4	r10i1181p1f1	2.03	-0.22
5	r9i1301p1f1	2.13	-0.80

Table 2: Difference in temperature (T) and relative humidity (RH) between 318
mid-century (2035-2065) and historic (1985-2015) of the five LENS2 ensemble 319
members used to generate decarbonization pathways. Index indicates the 1-5 320
label for each pathway that we use when presenting our results. 321
322

323 **2.3 Decarbonization Pathways and Resource Adequacy**
 324 **under Potential Climate Realizations**

325 From our CEM, we obtain five decarbonization pathways, each planned for one
 326 of five sampled ensemble members. To understand the vulnerability of each
 327 decarbonization pathway to other potential ensemble members, we approxi-
 328 mate the resource adequacy of each decarbonization pathway against all 100
 329 ensemble members (or climate realizations) from LENS2. Because LENS2 pro-
 330 vides daily values, we are unable to quantify resource adequacy (RA) of the
 331 Western Interconnect at an hourly basis using a standard probabilistic RA
 332 model. Instead, we approximate resource adequacy by quantifying daily Sur-
 333 plus Available Capacity (SAC) and Energy Not Served (ENS). While LENS2's
 334 daily resolution is a limitation of our study, LENS2 (and large ensembles gen-
 335 erally) provide unique insights into extremes of varying timescales, from daily
 336 extremes like extreme heat to longer extremes like droughts [55, 67].
 337

338 To calculate daily ENS, we run an economic dispatch model (EDM) for
 339 each decarbonization pathway output by our capacity expansion model in 2040.
 340 The EDM minimizes the sum of operating, CO₂ emission, inter-regional trans-
 341 mission, and ENS costs by optimizing generation, inter-regional transmission,
 342 and ENS decision variables. CO₂ emission costs include a decarbonization-
 343 pathway-specific CO₂ price necessary to achieve the relevant CO₂ emissions
 344 cap in that year. We determine this CO₂ price by iteratively increasing it
 345 until total CO₂ emissions comply with the cap. We include this price instead
 346 of a cap to avoid infeasibility in the EDM in climate realizations that pre-
 347 clude meeting the CO₂ cap. The EDM includes several constraints from the
 348 CEM, including balancing supply and demand within each of our five sub-
 349 regions while accounting for transmission inflows and outflows; constraining
 350 regional monthly hydropower generation to an energy budget; constraining
 351 wind and solar generation to spatially- and temporally-differentiated capacity
 352 factors; and constraining fossil-based thermal plant generation based on capac-
 353 ity deratings. Since we cannot probabilistically sample generator outages like
 354 hourly resource adequacy models, the EDM instead derates generators' capac-
 355 ities based on temperature-dependent or fixed forced outage rates (FORs). We
 356 run the EDM for a 1-year optimization horizon. Inputs to the EDM include
 357 a decarbonization pathway and variables driven by the given climate ensem-
 358 ble member (i.e., daily electricity demand, monthly hydroelectric generation,
 359 daily solar and wind capacity factors, and daily thermal plant forced outage
 360 rates and derates). See SI.F for the full EDM formulation and key parame-
 361 ters. The EDM is programmed in Python (3.10.6), the optimization problem
 362 is formulated with Pyomo (6.4.2) [68] and solved using GLPK 5.0 [69].

363 From the EDM output, we directly obtain daily ENS and calculate SAC for
 364 each region. SAC equals daily available non-hydropower capacity, hydropower
 365 generation, and transmission imports minus demand and transmission exports
 366 for each region. In this way, SAC indicates excess supply available in a region
 367 to satisfy unexpected increases in demand. The lower the SAC, the greater the
 368 risk of a supply shortfall, suggesting lower resource adequacy. Prior research

has used a net load metric as a proxy for resource adequacy [57, 70]. Our SAC extends the net load metric by capturing not just daily wind and solar generation potential, but also accounts for optimized hydroelectric dispatch; temperature dependent outages in thermal and hydroelectric power plants; capacity deratings in fossil-based thermal power plants; and electricity flows between regions. See SI.G for more details on SAC calculation.

2.4 LENS2 Climate Data and Conversion to Power System Variables

In the near-term (prior to 2050), internal variability (versus model or emissions scenario uncertainty) is the primary source of climate-related uncertainty [40, 42]. To capture the role of internal variability in driving potential climates through 2040, we use the CESM2 Large Ensemble (LENS2) [62]. This dataset is a single model initial-condition large ensemble (SMILE) following the SSP3-7.0 emissions trajectory. We treat this global emissions trajectory as independent of our system's emissions trajectory, as internal variability - not emissions uncertainty - is the primary source of uncertainty over our study period.

The LENS2 dataset consists of 100 ensemble members which are split into 2 groups each consisting of 50 realizations, where each group is driven by one forcing condition. Each of the 50 realizations in the two groups are initiated from different initial conditions sampled to reflect micro and macro perturbations in the pre-industrial control simulation. Unless noted otherwise, all the variables with a specified frequency represent an average over the inherent time periods, e.g. daily temperature is daily averaged temperatures and monthly runoffs are monthly averaged runoffs. We obtain daily surface temperature, 10m wind speed, surface downwelling solar flux, surface atmospheric pressure, surface relative humidity, and monthly total runoff from 1980-2050 for each ensemble member. We obtain these variables at the highest spatial resolution possible, at a 100 km by 100 km grid. While this spatial and temporal resolution is lower than what is preferred for power system modeling, higher resolution climate datasets (e.g., from statistical or dynamical downscaling) often do not sample as large of a range of internal climate variability as LENS2 [64, 71, 72], particularly in the time-span of interest to us (through 2040) and when focusing on extreme events. On the other hand, this approach does not sample climate response uncertainty, i.e., how different climate models portray the future response to greenhouse gas forcing. We discuss the value of using a large ensemble like LENS2 and how it can assist creation of higher resolution products in our Discussion. More information on LENS2 and our used variables are in SI.B.

We apply a mean bias correction to LENS2 surface temperatures using surface temperatures from the ERA5 reanalysis data [73, 74]. To bias correct runoff for forecasting hydroelectric generation, we use a mean bias scaling method for each of the constituent drought regions [ref B.4]. More details on the bias correction methods are in SI.B.2. Other studies using large ensembles for quantifying climate impacts have also used such mean bias correction

415 methods [42]. We do not use more sophisticated bias correction methods like
 416 quantile mapping (QM) as it fits the distribution of projections to observations
 417 (historical climate), which may lead to loss of changes in internal variability
 418 in the projections. We do not find a strong bias in solar radiation, so we did
 419 not bias correct it. Though we identify biases in 10 m wind speeds relative to
 420 ERA5, wind power capacity factors derived from bias corrected wind speeds
 421 are much lower compared to other observational datasets. As a result, we use
 422 the native LENS2 wind speed data in our analysis.

423 We use different models to derive power system variables from LENS2
 424 data. We calculate daily solar and wind capacity factors for each LENS2 grid
 425 cell using deterministic equations (SI.B.3). We calculate monthly hydroelectric
 426 generation using a linear regression model using total runoff as the predictor
 427 variable. We obtain the model for each drought region in the Western US [75]
 428 by training observed hydroelectric generation [76] trained against ERA5 total
 429 runoff. We then forecast hydroelectric generation using bias corrected total
 430 runoff from the LENS2 data (SI.B.4). We calculate demand for each of our five
 431 subregions using a piecewise linear regression model using daily temperature as
 432 the predictor variable. The regression model is trained using observed demand
 433 data and ERA5 surface temperatures, so ignores technological or population
 434 changes (SI.C). We calculate temperature-dependent forced outage rates for
 435 thermal power plants using plant-type-specific relationships [77] (SI.D). We
 436 also calculate capacity deratings of fossil-based thermal power plants for each
 437 LENS2 grid cell using plant-type-specific relationships between deratings and
 438 air temperatures, relative humidity, and/or air pressure (SI.D).

439

440 3 Results

441

442 3.1 Capacity Investments across Decarbonization 443 Pathways

444

445 We first examine the five decarbonization pathways output by our capacity
 446 expansion model. In creating these pathways using five sampled LENS2 ensem-
 447 ble members rather than creating 100 pathways using each of the 100 LENS2
 448 ensemble members, we demonstrate the value of our framework in analyzing
 449 a limited number of alternatives generated by computationally complex plan-
 450 ning models, similar to how alternatives are incorporated in system planning in
 451 practice. Each pathway is defined by its "fleet" of energy generator types. Our
 452 pathways decarbonize primarily through investment in wind and solar capac-
 453 ity, but exhibit different levels of investment (Figure 2). Interconnect-wide
 454 solar and wind capacity increase from roughly 40 and 30 GW in 2022, respec-
 455 tively, to up to 129 and 46 GW in 2040, respectively, across pathways. Between
 456 pathways, wind and solar capacities in 2040 range from 34 to 46 GW and
 457 from 103 to 129 GW, respectively. Small amounts (less than 4 GW) of NGCC
 458 with carbon capture and sequestration (CCS) are also deployed in four decar-
 459 bonization pathways. Heterogeneity in solar and natural gas capacity largely
 460 drives differences in total installed capacity between pathways, which ranges

from 252 to 280 GW. Solar capacity investment largely occurs in three regions - California, Desert Southwest, and Central - with high quality solar resources, while wind investment largely occurs in the Northwest, which has high quality wind resources (Figure A.1). No investment in interregional transmission beyond existing capacity occurs. Growth in wind, solar, and NGCC capacity displace other capacity, including coal-fired capacity, and replace lost capacity from the retirement of the Diablo Canyon nuclear generating station, which is located in California. Generation by plant type follows similar trends as capacity investments. Across pathways, wind, solar, natural gas, and hydropower account for roughly 7-13%, 31-37%, 23-27%, and 20-24% of annual generation, respectively, in 2040.

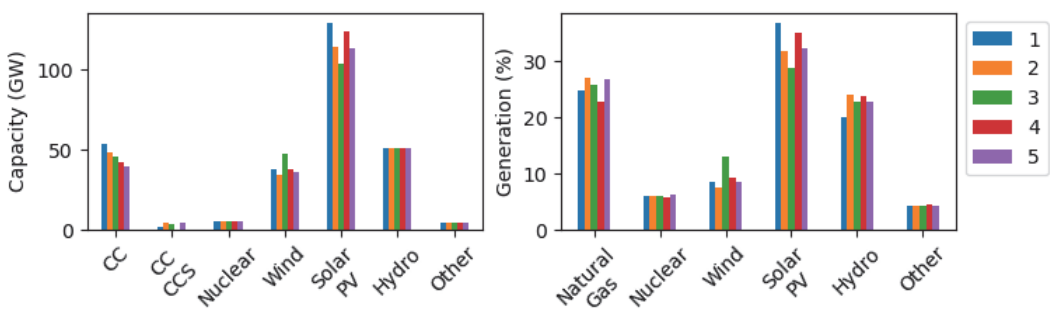


Fig. 2: (a) Installed capacity and (b) electricity generation by generator type across Western Interconnect in 2040 for each of our five decarbonization pathways (Table 2). CC stands for natural gas combined cycle, CCCS for CC with carbon capture and sequestration, and PV for photovoltaic. Other includes biomass, geothermal, landfill gas, and fossil and non-fossil waste plants.

3.2 Resource Adequacy of Decarbonization Pathways under Future Climate Realizations

For each decarbonization pathway, we use LENS2 to quantify daily electricity supply and demand under 100 potential climate realizations in any given year. Using daily supply and demand, we approximate resource adequacy through two metrics: daily surplus available capacity (SAC) and daily energy not served (ENS), both quantified in units of electricity. SAC indicates excess electricity supply available in a region to satisfy unexpected increases in demand, while ENS equals the difference between electricity demand and supply. A negative daily SAC value indicates ENS occurs, while larger positive SAC values indicate greater redundancy against supply shortfalls. ENS is rare in power systems, as it results in voluntary or involuntary load shedding. Involuntary load shedding occurs during rolling blackouts. Given daily SAC and ENS for each of our five decarbonization pathways under each of our 100 ensemble members, we then calculate the annual minimum SAC (“minimum SAC”), which

507 indicates the fleet's largest susceptibility to supply shortfalls in a given year,
508 and total annual ENS ("total ENS"), which indicates the fleet's total supply
509 shortfall in a given year.

510 Figures 3 and A.2 show these two metrics for the regions in the West-
511 ern Interconnect in 2040. Depending on the region, resource adequacy failures
512 occur in most or all decarbonization pathways under many climate realizations,
513 as indicated by negative SAC values and positive total ENS values. Pathways
514 exhibit significant differences in resource adequacy under future climate real-
515 izations. For instance, in California in 2040, one decarbonization pathway (5,
516 or the pathway generated using the r9i1301 climate ensemble member) has
517 a maximum of 286 GWh of total yearly ENS, whereas the other pathways
518 have maximum total yearly ENS of 0-100 GWh, respectively. The pathway
519 with the least ENS and greatest SAC - r10i1191 (or 1 in figure 5)- achieves
520 more installed capacity in 2040 (280 GW) relative to other pathways (251 -
521 262 GW), particularly through greater investment in solar PV and natural
522 gas combined cycle (Figure 2). Across decarbonization pathways, certain cli-
523 mate realizations incur significantly greater ENS than others (as indicated by
524 vertical red stripes). For instance, of the total ENS across all 2040 California
525 pathways and all 100 climate realizations, none of that ENS occurs in 79%
526 of climate realizations, while 50% of that ENS occurs in just 3% of climate
527 realizations. Maximum ENS values are driven by days with low hydropower,
528 coinciding low wind and solar generation, and high electricity demand (Figures
529 A.4 - A.8), indicating an important role of compounding extremes in driving
530 resource adequacy failures [22, 78].

531

532

533

534

535

536

537

538

539

540

541

542

543

544

545

546

547

548

549

550

551

552

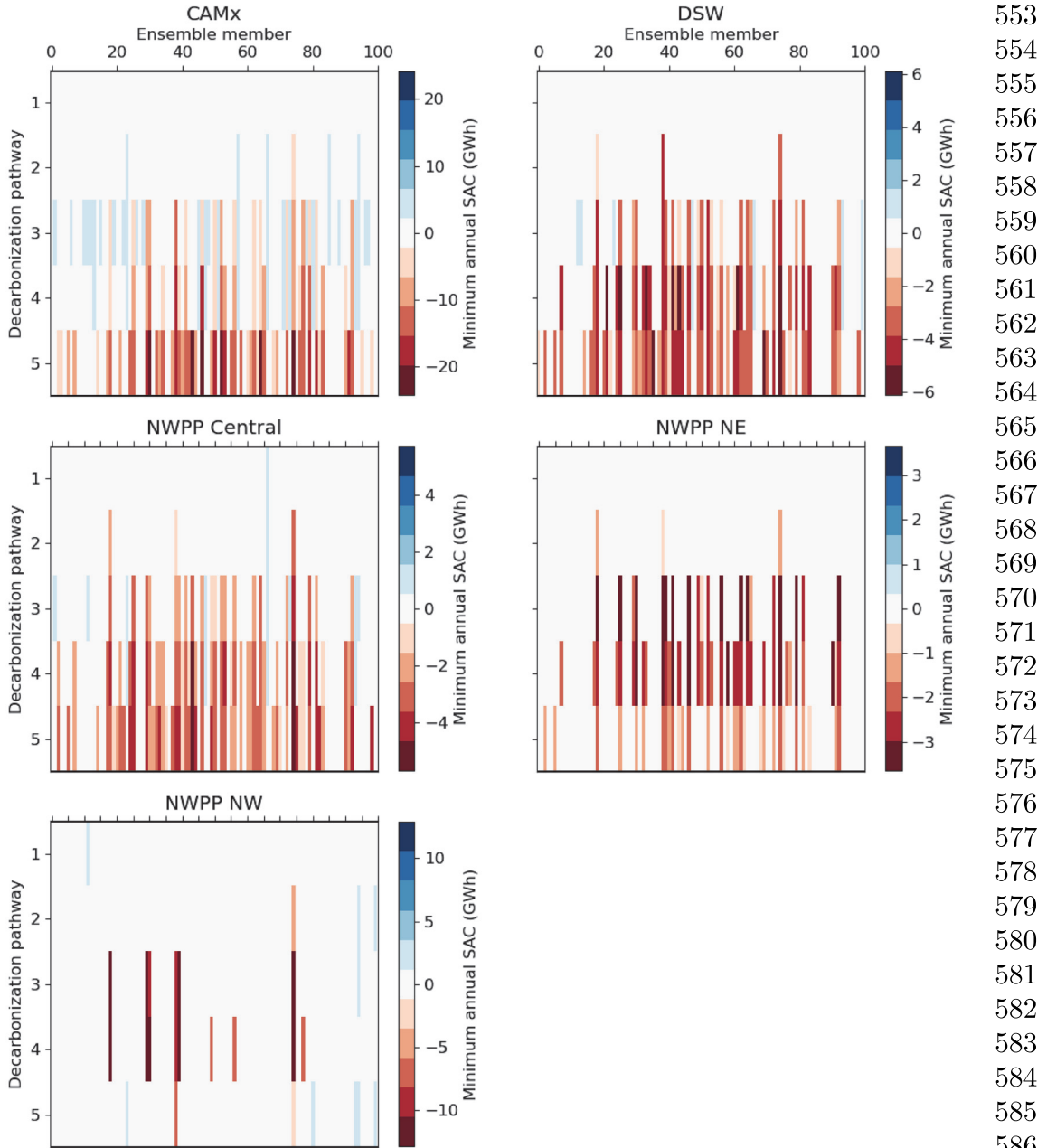


Fig. 3: Minimum annual SAC values for each subregion in 2040 (see Fig. 1 for map of regions). Each panel corresponds to a realization of the “Surplus available capacity” panel of Fig. 1. Each row corresponds to one of our five decarbonization pathways. Within each row, there are 100 separate color bars that indicate that pathway’s minimum annual SAC against each of our 100 climate ensemble members. Minimum annual SAC values range from negative (red) to positive (blue) red values indicate supply shortfalls (or resource adequacy failures), while blue values indicate surplus capacity relative to demand.

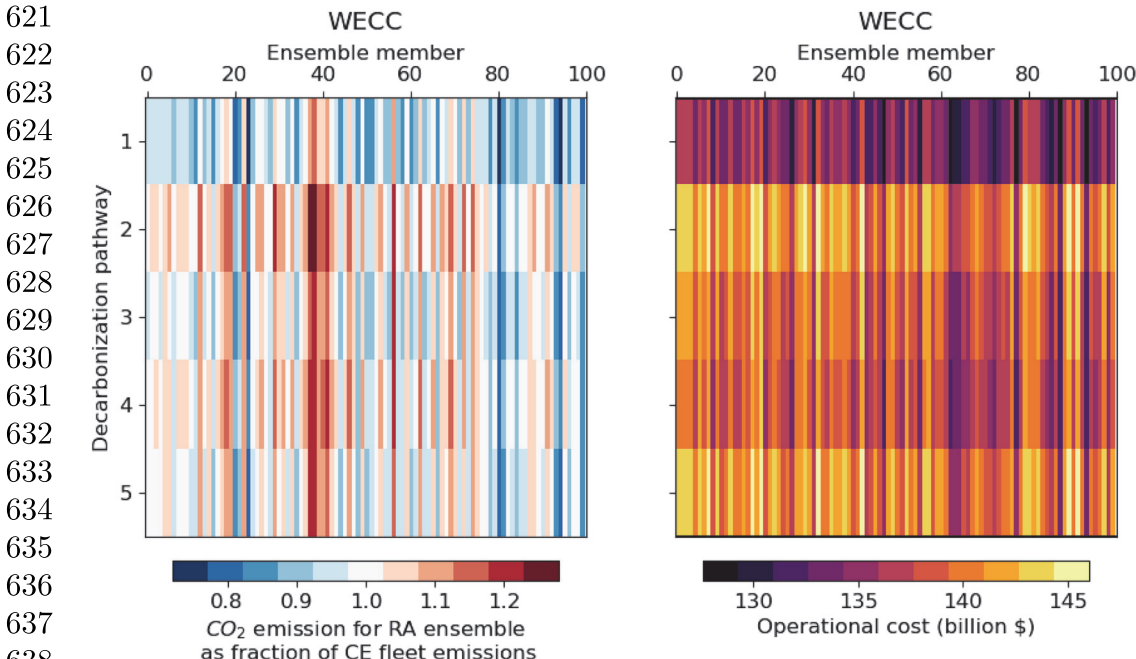
587
588
589
590
591
592
593
594
595
596
597
598

599 **3.3 Carbon Dioxide Emissions and Costs of**
 600 **Decarbonization Pathways under Climate**
 601 **Realizations**
 602

603 Future climate variability will affect not only the resource adequacy of future
 604 fleets, but also their CO₂ emissions and operational costs through changes
 605 in electricity demand; available wind, solar, and hydropower potential; and
 606 generation from dispatchable (largely fossil) plants (Figure 4). Across our
 607 decarbonization pathways, climate realizations could result in CO₂ emissions
 608 higher or lower than the CO₂ cap by up to 28% and 27%, respectively. As
 609 with resource adequacy (Figure 3), CO₂ emissions from some decarbonization
 610 pathways are less vulnerable to climate variability than others. For instance,
 611 one pathway (2, or generated using the r5i1231 climate ensemble member) fails
 612 to meet the CO₂ emissions cap in 70% of climate realizations, while another
 613 pathway (1) only fails to meet the emissions cap in 20% of realizations. Oper-
 614 615 tional costs also vary across climate realizations in each pathway, from \$127
 616 to \$146 billion. No single meteorological variable drives the observed variabil-
 617 ity in emissions and costs (Figure A.9). Rather, high emissions generally occur
 618 in climate realizations with low wind, solar, and hydropower generation and
 619 high demand.

620

621



639 **Fig. 4:** Same structure as Figure 3, but each color bar shows interconnect-
 640 wide CO₂ emissions as a fraction of the target CO₂ emissions cap (left) or
 641 interconnect-wide operational costs (right) in 2040.

642

643

644

3.4 Trade-offs between Resource Adequacy and Costs	645
Power system planners must balance competing objectives of minimizing system costs while meeting resource adequacy targets. Figure 5 compares each decarbonization pathway's total costs against the sum of annual minimum SAC over the five sub-regions (Figure 3) across 2040 climate realizations. Total costs include fixed investment costs, which vary between decarbonization pathways but not climate realizations, and operational costs (Figure 4), which vary between decarbonization pathways and climate realizations. Cumulative total costs from 2023 to 2040 range from \$223-246 billion across pathways and climate variability. Although pathways are differentiated by their mean costs across realizations, variability in operational costs induced by climate variability introduces overlap in total cost ranges between pathways. Despite overlaps between total costs, pathways can exhibit significant differences in resource adequacy outcomes. For instance, one pathway (1, or the first pathway from the right in Figure 5) only exhibits a small resource adequacy failure (or a total regional minimum annual SAC value of -0.2 GWh) under one climate realization, and has a positive mean SAC value across ensemble members. Other pathways (e.g., the three pathways at left in Figure 5) have larger resource adequacy failures (of up to -40 GWh SAC) under certain ensemble members, and negative mean SAC values across ensemble members (of up to -10 GWh). Selecting the first pathway rather than other pathways would eliminate resource adequacy failures at a median total cost difference of -1 to 3%.	646 647 648 649 650 651 652 653 654 655 656 657 658 659 660 661 662 663 664 665 666 667 668
3.5 Identifying an Alternative Decarbonization Pathway Robust to Future Climate Realizations	669 670 671
Our prior results indicate a subset of potential climate realizations drive significant risk of resource adequacy failures across decarbonization pathways (Figure 3). We identify the ensemble member that drives the largest resource adequacy failures (quantified as the sum of minimum annual SACs) across decarbonization pathways in California (our largest load region) in 2040, namely r19i1231 (or pathway 6), then rerun our capacity expansion model using that ensemble member's meteorology. This ensemble member was not captured in our initial sampling procedure, in which we selected five ensemble members that spanned the warming at mid-century represented by the ensembles in the CESM2-LE dataset (Figure B.1). Rather, r19i1231 features a compound extreme event in 2040 of low hydropower and wind generation potential and high air temperatures, the latter of which drive elevated electricity demand and low available thermal capacity (Figure A.11). Capturing unexpected extreme climate realizations, such as r19i1231, is a key motivator for our framework, as identifying extremes a priori is difficult given complex interactions within power systems.	672 673 674 675 676 677 678 679 680 681 682 683 684 685 686
Our new decarbonization pathway generated with the r19i1231 climate ensemble member invests in more solar and NGCC capacity and in less wind capacity than other pathways (Figure 6a). Overall, capacity investment is 2 to 30 GW greater in the new pathway than other pathways. Figure 6b compares	687 688 689 690

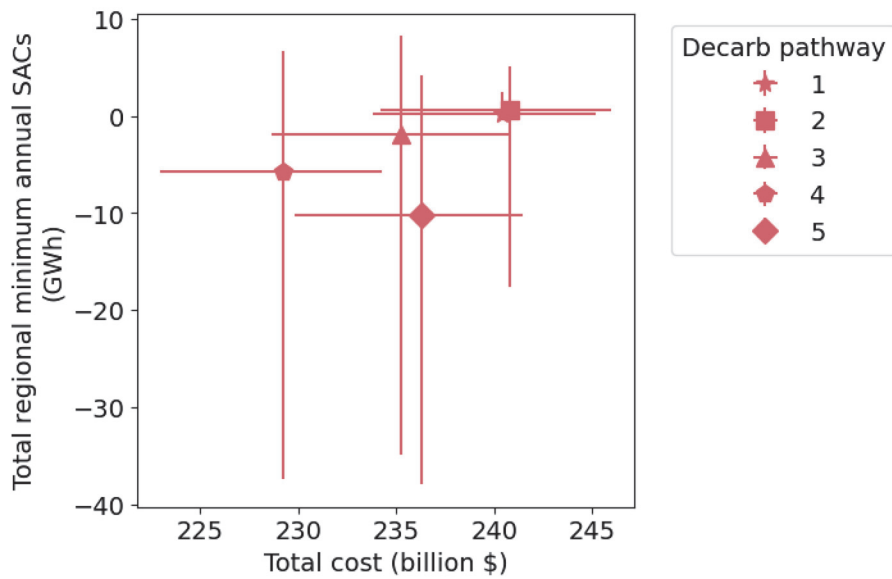


Fig. 5: Sum of minimum annual SAC values for our five subregions in 2040 versus cumulative (2023-2040) total (fixed plus operating) costs for each decarbonization pathway. Minimum annual SAC values equal the sum of non-synchronous subregional minimum SAC values. Each decarbonization pathway is depicted with a cross; the dot at the center of each cross indicates the mean total SAC and mean total cost for that decarbonization pathway across all 100 climate ensemble members; the horizontal arm of each cross ranges from the minimum to maximum total cost for that decarbonization pathway across all 100 climate ensemble members; and the vertical arm of each cross ranges from the minimum to maximum total SACs for that decarbonization pathway across all 100 climate ensemble members. For context, total non-synchronous peak demand across the five subregions equals roughly 200 GWh (although peak demand varies across climate realizations). A negative minimum annual SAC value indicates one or more subregions in that pathway experiences a supply shortfall under at least one future climate realization.

the resource adequacy of the decarbonization pathway generated with this new ensemble member versus our original decarbonization pathways. Our new pathway exhibits significantly higher minimum SAC values, indicating less vulnerability to resource adequacy failures. In fact, the new pathway does not experience any resource adequacy failures across any climate realizations in 2040 in any region (i.e., no ENS or negative SAC values), and has a minimum annual SAC of 0-3 GWh in California across climate realizations. The newly generated pathway also meets CO₂ emission caps in all but three potential climate realizations (Figure 6c). Figure 6d compares the trade-off between resource adequacy and system costs for the new versus prior pathways. The new pathway has significantly better resource adequacy than prior pathways, but at greater total costs. Specifically, the new pathway incurs, on average,

roughly \$10 billion greater total costs between 2023 and 2040 compared to the next costliest pathway.

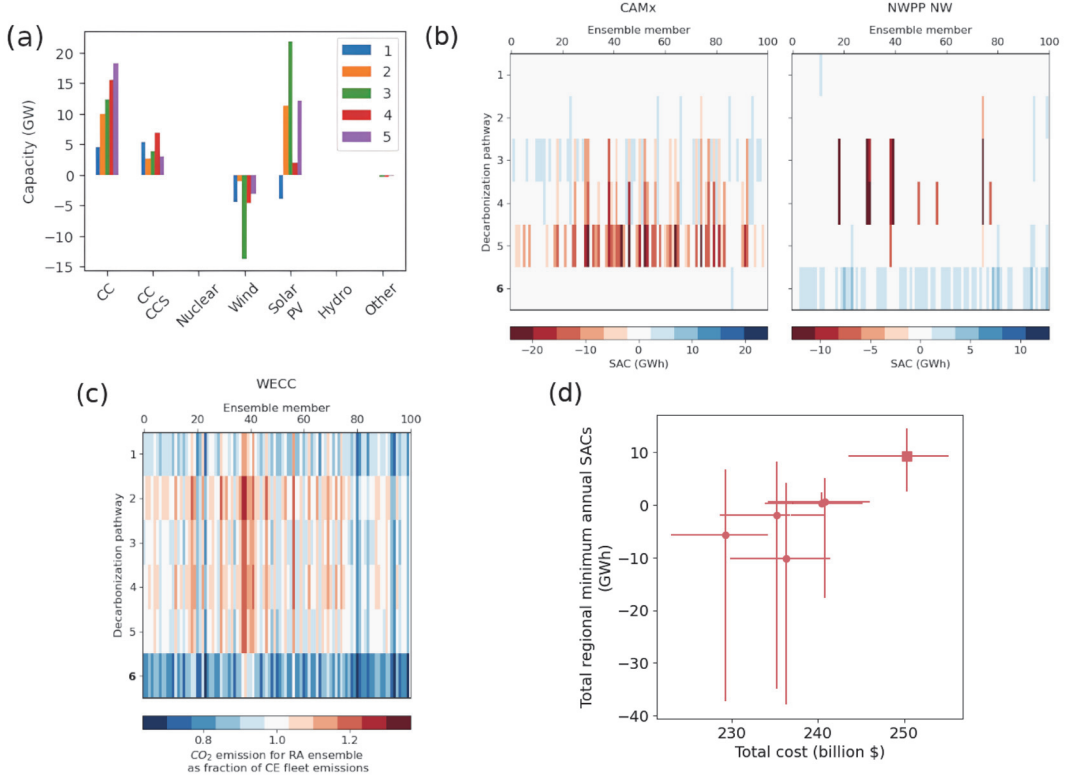


Fig. 6: (a) Difference in installed capacity by generator type across Western Interconnect in 2040 between the decarbonization pathway generated using the r19i1231 ensemble member (pathway "6") and each of the other decarbonization pathways. CC stands for natural gas combined cycle, CCCS for CC with carbon capture and sequestration, and PV for photovoltaic. (b) Same structure as Figure 3, but includes the decarbonization pathway generated using the r19i1231 ensemble member (pathway "6") and only includes the two largest subregions by demand for conciseness. (c) Same structure as left panel of Figure 4, but includes the decarbonization pathway generated using the r19i1231 ensemble member (pathway "6") (bolded at top). (d) Same structure as Figure 5, but includes the decarbonization pathway generated using the r19i1231 ensemble member (shown as cross centered on square instead of circle).

4 Discussion

Existing research and system planning practices lack decision support frameworks for identifying investment alternatives that are robust to climate-related uncertainty. We construct such an analytical framework by integrating planning and operational power system models with a large climate ensemble, then

737
738
739
740
741
742
743
744
745
746
747
748
749
750
751
752
753
754
755
756
757
758
759
760

761
762
763
764
765
766
767
768
769
770
771
772
773
774
775
776
777
778
779
780
781
782

783 use our framework to identify the vulnerabilities, trade-offs, and robustness
784 of alternative decarbonization pathways for the Western U.S. power system
785 in 2040. We began our analysis with five alternative pathways to 60% decar-
786 bonization of the power system. All of these pathways exhibited modest to
787 significant resource adequacy failures under potential climate realizations. But
788 by choosing one pathway over others, significantly better resource adequacy
789 outcomes can be achieved at little additional cost. Even this more robust
790 pathway, though, suffered resource adequacy losses under future climate real-
791 izations. By identifying a particularly problematic future climate realization
792 for future resource adequacy and using it to create another alternative decar-
793 bonization pathway, we identified a pathway robust to, or that experienced
794 no resource adequacy failures under, all examined future climate realizations.
795 This robustness is achieved through an increase of roughly \$10 billion (or 5%)
796 in total costs, posing a trade-off to decision-makers.

797 Our analysis quantifies the resource adequacy of alternative decarboniza-
798 tion pathways against a wide range of near-term climate variability. Capturing
799 this range of climate variability was possible through the use of the LENS2
800 dataset, but came at the cost of climate data with poor spatial and tempo-
801 ral resolution. Energy system modeling needs and available climate dataset
802 characteristics are often misaligned [25], and conducting detailed downscaling
803 of all LENS2 ensemble members is computationally prohibitive. However, our
804 analytical framework can guide high resolution downscaling of large climate
805 ensembles like LENS2 for energy system applications, a key need for energy
806 system modelers. Specifically, our framework can identify ensemble members,
807 periods of interest, and/or climate conditions that pose the greatest threat
808 to alternative future power systems. Threatening conditions are themselves a
809 function of investment decisions in power systems, so identifying those con-
810 ditions for a broad range of alternatives, as our framework enables, is crucial
811 to fully characterize vulnerabilities and robustness. In our case, one ensem-
812 ble member (r19i1231) resulted in resource adequacy failures across nearly all
813 studied decarbonization targets due to the compounding effects of low wind
814 and hydropower generation potential and high air temperatures. Identified
815 members, periods, or climate conditions of concern can be selectively down-
816 scaled and fed back into planning or resource adequacy modeling, maximizing
817 the value of high resolution downscaled data. This process requires bottom-up
818 trans-disciplinary collaboration between energy system and climate modellers
819 [25].

820 In using climate data with poor temporal (daily) resolution, our analysis
821 suffers from two shortfalls. First, we are unable to capture the diurnal pattern
822 of solar power in which it does not generate power at night, potentially bias-
823 ing our investment decisions and resource adequacy analyses in favor of solar
824 power. Second, because we do not resolve periods within the day, we are unable
825 to include intra-day electricity storage in our planning or resource adequacy
826 modeling. Intra-day storage, particularly utility-scale lithium-ion facilities, is a
827
828

rapidly growing source of grid capacity and flexibility, particularly in California [79, 80]. This flexibility and capacity could provide valuable when adapting to climate change and increasing intensity and frequency of extreme weather events. While our LENS2 climate dataset is unable to capture this value, implementation of our framework per the above guidelines would enable stakeholders to capture the value of storage for climate adaptation. Daily resolution could also explain the lack of investment in interregional transmission capacity, since short-term (sub-daily) peaks in wind and solar generation drive value for expanded inter-regional transmission. Prior research on decarbonization scenarios for the Western United States using high resolution historic weather data finds significant transmission expansion in cost-optimal futures [8, 81].

Additional opportunities for extending our research exist. We do not consider changes in demand due to adoption of new technologies, e.g. heat pumps to electrify space heating or space cooling in response to increasing temperatures. In winter peaking regions like the Northwest, electrified heating through heat pumps can lead to higher demand in the winter months, introducing interactions between decarbonization and climate change that could affect our SAC calculations. In the Northwest and other regions with historically low space cooling penetrations, adoption of space cooling could also interact with increasing extreme heat to exacerbate summer peak demands. Incorporating the effect of such demand-side changes in our models will allow us to make accurate assessment of future fleets' robustness [9]. Future research could also extend our framework to incorporate additional robustness concepts. For instance, in practice utilities design future systems that meet certain resource adequacy thresholds, e.g. the 1-in-10 standard, which could be captured using a satisficing metric. While we focus on the year 2040 when assessing resource adequacy of alternative systems against potential climate realizations, future research could also consider the temporal evolution of system outcomes under climate change. Doing so could illuminate trade-offs in the near- to long-term of decarbonization pathways to climate change. Our framework could also be extended to planning of other power systems in the United States and globally, which will also grapple with climate-change-driven impacts on demand and supply [82]. Specific insights, though, will vary given region-specific contexts that will moderate impacts of climate change, e.g. regions will vary in their reliance on hydropower and need for space heating and/or cooling.

Our framework provides a practical way for real-world system planners and utilities to better account for climate-related uncertainty, whether planning for individual or multiple regions in the Western United States or elsewhere. Regulators could also require system planners to use our framework during Integrated Resource Plan (IRP) proceedings to understand trade-offs between improved resource adequacy and greater consumer costs. Many system planners use third-party software, e.g. PLEXOS, to make long-term plans. Modifying the underlying mathematical formulation of such software is challenging for end users. Instead, our framework requires changes to model inputs and additional processing of model results, a more feasible undertaking. The

829
830
831
832
833
834
835
836
837
838
839
840
841
842
843
844
845
846
847
848
849
850
851
852
853
854
855
856
857
858
859
860
861
862
863
864
865
866
867
868
869
870
871
872
873
874

875 key element of our analytical approach is to stress test alternative investment
876 plans (or decarbonization pathways) against potential climate realizations to
877 identify system vulnerabilities and challenging climate conditions, then feed
878 identified challenging conditions back into decisionmaking. Energy system
879 planners will use planning processes that diverge from our methods in sev-
880 eral ways. Despite these differences, planners can adopt the key element of our
881 analysis into their planning processes to better deal with climate-related uncer-
882 tainty by following these guidelines. First, planners should identify a range of
883 climate realizations of interest, ideally in collaboration with climate scientists.
884 These realizations will likely have higher resolution than our LENS2 climate
885 dataset, requiring planners to sample periods to include in their planning
886 model given computational constraints. Planners can adapt their sampling
887 procedures or adopt new procedures designed for future climate data [83]. In
888 either case, sampled time periods will not capture the full range of weather
889 conditions that could affect future power systems. Stress testing alternative
890 decarbonization pathways to the full range of weather, the key element of our
891 framework, can therefore generate crucial insights into system vulnerability
892 when sampling time periods for planning. Second, planners should analyze
893 alternative decarbonization pathways that stem not from climate variability,
894 but instead from other sources of uncertainty that they typically focus on, e.g.
895 policy, emissions reduction target, or technology availability. With our frame-
896 work, planners can understand vulnerabilities of these alternative pathways to
897 future climate change. Third, planners can feed identified vulnerabilities and
898 meteorological drivers of those vulnerabilities back into their planning pro-
899 cess, e.g. as additional sampled periods, to identify more robust investment
900 strategies. Finally, our framework can illuminate investment pathways robust
901 to climate change, but investment strategies should be coupled with adaptive
902 planning [34] to ensure continued robustness under climate uncertainty. By
903 following these guidelines, our framework can help stakeholders identify future
904 power systems that are robust to climate change and that simultaneously
905 advance reliable, affordable, and clean objectives.

906

907

908 **5 Acknowledgements**

909

910 Michael Craig and Srihari Sundar thank the U.S. National Science Founda-
911 tion under Award Number 2142421 for funding this work. They thank the
912 CESM2 Large Ensemble Community Project and supercomputing resources
913 provided by the IBS Center for Climate Physics in South Korea. They also
914 thank the high-performance computing support for the use of Casper clus-
915 ter provided by NCAR’s Computational and Information Systems Laboratory,
916 sponsored by the National Science Foundation. Flavio Lehner acknowledges
917 support from the U.S. Department of Energy, Office of Science, Office of Bio-
918 logical & Environmental Research (BER), Regional and Global Model Analysis
919 (RGMA) component of the Earth and Environmental System Modeling Pro-
920 gram under Award Number DE-SC0022070 and National Science Foundation

(NSF) IA 1947282. The National Center for Atmospheric Research is sponsored by the National Science Foundation. Nathalie Voisin was supported by the GODEEEP Investment at Pacific Northwest National Laboratory (PNNL). PNNL is a multi-program national laboratory operated for the U.S. Department of Energy (DOE) by Battelle Memorial Institute under Contract No. DE-AC05-76RL01830. The views and opinions of authors expressed herein do not necessarily state or reflect those of the United States Government or any agency thereof. Many visualizations were created with Seaborn [84] and SS thanks the developers of this and many other open source packages

6 Data availability

Meteorological data used in this study is available through [62]. Code for the CEM, SAC calculations, and analysis notebook used to create figures in the manuscript are available at <https://github.com/ASSET-Lab/WesternUSRDM>. Processed meteorological fields and data used in the analysis will be archived in Zenodo. Analysis data is available temporarily at WesternUSRDM-drive.

References

- [1] Clarke, L., Wei, Y.-M., Navarro, A.D.L.V., Garg, A., Hahmann, A.N., Khennas, S., Azevedo, I.M.L., Löschel, A., Singh, A.K., Steg, L., Strbac, G., Wada, K.: Energy Systems. In: Shukla, P.R., Skea, J., Slade, R., Khourdajie, A.A., van Diemen, R., McCollum, D., Pathak, M., Some, S., Vyas, P., Fradera, R., Belkacemi, M., Hasija, A., Lisboa, G., Luz, S., Malley, J. (eds.) IPCC, 2022: Climate Change 2022: Mitigation of Climate Change. Contribution of Working Group III to the Sixth Assessment Report of the Intergovernmental Panel on Climate Change. Cambridge University Press, Cambridge, UK and New York, NY, USA (2022). Chap. 6. <https://doi.org/10.1017/9781009157926.008> 942
- [2] Rogelj, J., Schaeffer, M., Meinshausen, M., Knutti, R., Alcamo, J., Riahi, K., Hare, W.: Zero emission targets as long-term global goals for climate protection. *Environmental Research Letters* **10**(10), 105007 (2015) 953
- [3] National Academies of Sciences, Engineering, and Medicine, et al.: Accelerating decarbonization of the us energy system (2021) 957
- [4] Jenkins, J.D., Mayfield, E.N., Farbes, J., Jones, R., Patankar, N., Xu, Q., Schivley, G.: Preliminary report: The climate and energy impacts of the inflation reduction act of 2022. REPEAT Project, Princeton, NJ (2022) 960
- [5] Ralston Fonseca, F., Craig, M., Jaramillo, P., Bergés, M., Severnini, E., Loew, A., Zhai, H., Cheng, Y., Nijssen, B., Voisin, N., Yearsley, J.: Effects of Climate Change on Capacity Expansion Decisions of an Electricity 964

967 Generation Fleet in the Southeast U.S. Environ. Sci. Technol. (2021).
968 <https://doi.org/10.1021/acs.est.0c06547>

969

970 [6] Denholm, P., Brown, P., Cole, W., Mai, T., Sergi, B., Brown, M., Jadun,
971 P., Ho, J., Mayernik, J., McMillan, C., Sreenath, R.: Examining supply-
972 side options to achieve 100% clean electricity by 2035 (2022)

973

974 [7] Cole, W., Carag, J.V., Brown, M., Brown, P., Cohen, S., Eurek, K., Fra-
975 zier, W., Gagnon, P., Grue, N., Ho, J., Lopez, A., Mai, T., Mowers,
976 M., Murphy, C., Sergi, B., Steinberg, D., Williams, T.: 2021 standard
977 scenarios report: A u.s. electricity sector outlook. NREL (2021). <https://doi.org/10.2172/1834042>

978

979 [8] Jenkins, J.D., Mayfield, E.N., Larson, E.D., Pacala, S.W., Greig, C.: Mis-
980 sion net-zero america: The nation-building path to a prosperous, net-zero
981 emissions economy. Joule 5(11), 2755–2761 (2021)

982

983 [9] Wessel, J., Kern, J.D., Voisin, N., Oikonomou, K., Haas, J.: Tech-
984 nology pathways could help drive the us west coast grid's exposure
985 to hydrometeorological uncertainty. Earth's Future 10(1), 2021–002187
986 (2022)

987

988 [10] Davis, S.J., Lewis, N.S., Shaner, M., Aggarwal, S., Arent, D., Azevedo,
989 I.L., Benson, S.M., Bradley, T., Brouwer, J., Chiang, Y.-M., *et al.*: Net-
990 zero emissions energy systems. Science 360(6396), 9793 (2018)

991

992 [11] Berrill, P., Wilson, E.J., Reyna, J.L., Fontanini, A.D., Hertwich, E.G.:
993 Decarbonization pathways for the residential sector in the united states.
994 Nature Climate Change 12(8), 712–718 (2022)

995

996 [12] Lee, H., Calvin, K., Dasgupta, D., Krinner, G., Mukherji, A., Thorne, P.:
997 Synthesis report of the ipcc sixth assessment report (ar6). Intergovern-
998 mental Panel on Climate Change, Geneva, Switzerland [Google Scholar]
999 (2023)

1000

1001 [13] Craig, M.T., Cohen, S., Macknick, J., Draxl, C., Guerra, O.J., Sengupta,
1002 M., Haupt, S.E., Hodge, B.-M., Brancucci, C.: A review of the potential
1003 impacts of climate change on bulk power system planning and operations
1004 in the united states. Renewable and Sustainable Energy Reviews 98, 255–
1005 267 (2018)

1006

1007 [14] Auffhammer, M., Baylis, P., Hausman, C.H.: Climate change is projected
1008 to have severe impacts on the frequency and intensity of peak electricity
1009 demand across the united states. Proceedings of the National Academy
1010 of Sciences 114(8), 1886–1891 (2017)

1011

1012

- [15] Ralston Fonseca, F., Jaramillo, P., Bergés, M., Severnini, E.: Seasonal effects of climate change on intra-day electricity demand patterns. *Climatic Change* **154**, 435–451 (2019) 1013
1014
1015
1016
- [16] Miara, A., Macknick, J.E., Vörösmarty, C.J., Tidwell, V.C., Newmark, R., Fekete, B.: Climate and water resource change impacts and adaptation potential for us power supply. *Nature Climate Change* **7**(11), 793–798 (2017) 1017
1018
1019
1020
1021
- [17] Henry, C.L., Pratson, L.F.: Effects of environmental temperature change on the efficiency of coal-and natural gas-fired power plants. *Environmental science & technology* **50**(17), 9764–9772 (2016) 1022
1023
1024
- [18] Bartos, M.D., Chester, M.V.: Impacts of climate change on electric power supply in the western united states. *Nature Climate Change* **5**(8), 748–752 (2015) 1025
1026
1027
1028
- [19] Karnauskas, K.B., Lundquist, J.K., Zhang, L.: Southward shift of the global wind energy resource under high carbon dioxide emissions. *Nature Geoscience* **11**(1), 38–43 (2018) 1029
1030
1031
1032
- [20] Turner, S.W., Ng, J.Y., Galelli, S.: Examining global electricity supply vulnerability to climate change using a high-fidelity hydropower dam model. *Science of the Total Environment* **590**, 663–675 (2017) 1033
1034
1035
1036
- [21] Schewe, J., Heinke, J., Gerten, D., Haddeland, I., Arnell, N.W., Clark, D.B., Dankers, R., Eisner, S., Fekete, B.M., Colón-González, F.J., *et al.*: Multimodel assessment of water scarcity under climate change. *Proceedings of the National Academy of Sciences* **111**(9), 3245–3250 (2014) 1037
1038
1039
1040
1041
1042
- [22] Turner, S.W.D., Voisin, N., Fazio, J., Hua, D., Jourabchi, M.: Compound climate events transform electrical power shortfall risk in the Pacific Northwest. *Nat. Commun.* **10**(1) (2019). <https://doi.org/10.1038/s41467-018-07894-4> 1043
1044
1045
1046
1047
- [23] Ralston Fonseca, F., Craig, M., Jaramillo, P., Bergés, M., Severnini, E., Loew, A., Zhai, H., Cheng, Y., Nijssen, B., Voisin, N., *et al.*: Climate-induced tradeoffs in planning and operating costs of a regional electricity system. *Environmental Science & Technology* **55**(16), 11204–11215 (2021) 1048
1049
1050
1051
1052
- [24] Sundar, S., Craig, M.T., Payne, A.E., Brayshaw, D.J., Lehner, F.: Meteorological drivers of resource adequacy failures in current and high renewable western us power systems. *Nature Communications* **14**(1), 6379 (2023) 1053
1054
1055
1056
1057
1058

1059 [25] Craig, M.T., Wohland, J., Stoop, L.P., Kies, A., Pickering, B., Bloom-
1060 field, H.C., Browell, J., De Felice, M., Dent, C.J., Deroubaix, A., *et al.*:
1061 Overcoming the disconnect between energy system and climate modeling.
1062 Joule **6**(7), 1405–1417 (2022)
1063

1064 [26] Bloomfield, H., Brayshaw, D., Troccoli, A., Goodess, C., De Felice,
1065 M., Dubus, L., Bett, P., Saint-Drenan, Y.-M.: Quantifying the sensitiv-
1066 ity of european power systems to energy scenarios and climate change
1067 projections. Renewable Energy **164**, 1062–1075 (2021)
1068

1069 [27] Abdin, I., Fang, Y.-P., Zio, E.: A modeling and optimization framework
1070 for power systems design with operational flexibility and resilience against
1071 extreme heat waves and drought events. Renewable and Sustainable
1072 Energy Reviews **112**, 706–719 (2019)
1073

1074 [28] Simoes, S.G., Amorim, F., Siggini, G., Sessa, V., Saint-Drenan, Y.-M.,
1075 Carvalho, S., Mraihi, H., Assoumou, E.: Climate proofing the renewable
1076 electricity deployment in europe-introducing climate variability in large
1077 energy systems models. Energy Strategy Reviews **35**, 100657 (2021)
1078

1079 [29] Santos da Silva, S.R., Hejazi, M.I., Iyer, G., Wild, T.B., Binsted, M.,
1080 Miralles-Wilhelm, F., Patel, P., Snyder, A.C., Vernon, C.R.: Power sector
1081 investment implications of climate impacts on renewable resources in latin
1082 america and the caribbean. Nature communications **12**(1), 1276 (2021)
1083

1084 [30] Kozarcanin, S., Liu, H., Andresen, G.B.: 21st century climate change
1085 impacts on key properties of a large-scale renewable-based electricity
1086 system. Joule **3**(4), 992–1005 (2019)
1087

1088 [31] Schlott, M., Kies, A., Brown, T., Schramm, S., Greiner, M.: The impact
1089 of climate change on a cost-optimal highly renewable european electricity
1090 network. Applied energy **230**, 1645–1659 (2018)
1091

1092 [32] Webster, M., Fisher-Vanden, K., Kumar, V., Lammers, R.B., Perla, J.:
1093 Integrated hydrological, power system and economic modelling of climate
1094 impacts on electricity demand and cost. Nature Energy **7**(2), 163–169
(2022)
1095

1096 [33] Weaver, C.P., Lempert, R.J., Brown, C., Hall, J.A., Revell, D., Sarewitz,
1097 D.: Improving the contribution of climate model information to decision
1098 making: the value and demands of robust decision frameworks. Wiley
1099 Interdisciplinary Reviews: Climate Change **4**(1), 39–60 (2013)
1100

1101 [34] Marchau, V.A., Walker, W.E., Bloemen, P.J., Popper, S.W.: Decision
1102 Making Under Deep Uncertainty: from Theory to Practice. Springer, ???
1103 (2019)
1104

[35] WG, I.: The physical science basis. Contribution of working group I to the fifth assessment report of the intergovernmental panel on climate change **1535** (2013) 1105
1106
1107
1108

[36] Hallegatte, S., Shah, A., Brown, C., Lempert, R., Gill, S.: Investment decision making under deep uncertainty—application to climate change. World Bank Policy Research Working Paper (6193) (2012) 1109
1110
1111
1112

[37] Fourth national climate assessment. Technical report, U.S. Global Change Research Program (2018). <https://nca2018.globalchange.gov> Accessed 2024-06-16 1113
1114
1115
1116

[38] Hawkins, E., Sutton, R.: The potential to narrow uncertainty in regional climate predictions. Bulletin of the American Meteorological Society **90**(8), 1095–1108 (2009) 1117
1118
1119

[39] Deser, C., Phillips, A., Bourdette, V., Teng, H.: Uncertainty in climate change projections: the role of internal variability. Climate dynamics **38**, 527–546 (2012) 1120
1121
1122
1123

[40] Lehner, F., Deser, C., Maher, N., Marotzke, J., Fischer, E.M., Brunner, L., Knutti, R., Hawkins, E.: Partitioning climate projection uncertainty with multiple large ensembles and cmip5/6. Earth System Dynamics **11**(2), 491–508 (2020) 1124
1125
1126
1127
1128

[41] Lehner, F., Deser, C.: Origin, importance, and predictive limits of internal climate variability. Environmental Research: Climate **2**(2), 023001 (2023) 1129
1130
1131

[42] Schwarzwald, K., Lenssen, N.: The importance of internal climate variability in climate impact projections. Proceedings of the National Academy of Sciences **119**(42), 2208095119 (2022) 1132
1133
1134
1135

[43] CPUC, CAISO, CEC: Root Cause Analysis: Mid-August 2020 Extreme Heat Wave (2021). <http://www.caiso.com/Documents/Final-Root-Cause-Analysis-Mid-August-2020-Extreme-Heat-Wave.pdf> 1136
1137
1138

[44] Mays, J., Craig, M.T., Kiesling, L., Macey, J.C., Shaffer, B., Shu, H.: Private risk and social resilience in liberalized electricity markets. Joule (2022) 1139
1140
1141
1142

[45] North American Electric Reliability Corporation: 2021 Long-Term Reliability Assessment (2021). <https://www.nerc.com/pa/RAPA/ra/Pages/default.aspx> 1143
1144
1145
1146

[46] Lempert, R.J.: Shaping the next one hundred years: New methods for quantitative, long-term policy analysis (2003) 1147
1148
1149
1150

1151 [47] Lempert, R.J., Groves, D.G.: Identifying and evaluating robust adaptive
1152 policy responses to climate change for water management agencies in the
1153 american west. *Technological Forecasting and Social Change* **77**(6), 960–
1154 974 (2010)

1155

1156 [48] Giuliani, M., Castelletti, A.: Is robustness really robust? how different
1157 definitions of robustness impact decision-making under climate change.
1158 *Climatic Change* **135**(3), 409–424 (2016)

1159

1160 [49] Fischbach, J.R., Siler-Evans, K., Tierney, D., Wilson, M.T., Cook, L.M.,
1161 May, L.W.: Robust stormwater management in the pittsburgh region.
1162 RAND Corporation (2017)

1163

1164 [50] Reis, J., Shortridge, J.E.: Impact of uncertainty parameter distribution
1165 on robust decision making outcomes for climate change adaptation under
1166 deep uncertainty. *Risk Analysis* **40**(3), 494–511 (2020)

1167

1168 [51] Shortridge, J.E., Guikema, S.D.: Scenario discovery with multiple criteria:
1169 An evaluation of the robust decision-making framework for climate change
1170 adaptation. *Risk Analysis* **36**(12), 2298–2312 (2016)

1171

1172 [52] Markolf, S.A., Hoehne, C., Fraser, A.M., Chester, M.V., Underwood, B.S.:
1173 Transportation resilience to climate change and extreme weather events—
1174 beyond risk and robustness. *Transport Policy* **74**, 174–186 (2019)

1175

1176 [53] Smith, R., Zagona, E., Kasprzyk, J., Bonham, N., Alexander, E., Butler,
1177 A., Prairie, J., Jerla, C.: Decision science can help address the challenges
1178 of long-term planning in the colorado river basin. *JAWRA Journal of the*
1179 *American Water Resources Association* **58**(5), 735–745 (2022)

1180

1181 [54] Nahmmacher, P., Schmid, E., Pahle, M., Knopf, B.: Strategies against
1182 shocks in power systems—an analysis for the case of europe. *Energy*
1183 *Economics* **59**, 455–465 (2016)

1184

1185 [55] Deser, C., Lehner, F., Rodgers, K.B., Ault, T., Delworth, T.L., DiNezio,
1186 P.N., Fiore, A., Frankignoul, C., Fyfe, J.C., Horton, D.E., *et al.*: Insights
1187 from earth system model initial-condition large ensembles and future
1188 prospects. *Nature Climate Change* **10**(4), 277–286 (2020)

1189

1190 [56] Maher, N., Milinski, S., Ludwig, R.: Large ensemble climate model simu-
1191 lations: introduction, overview, and future prospects for utilising multiple
1192 types of large ensemble. *Earth System Dynamics* **12**(2), 401–418 (2021)

1193

1194 [57] van der Wiel, K., Stoop, L.P., Van Zuijlen, B., Blackport, R., Van den
1195 Broek, M., Selten, F.: Meteorological conditions leading to extreme low
1196 variable renewable energy production and extreme high energy shortfall.
Renewable and Sustainable Energy Reviews **111**, 261–275 (2019)

[58] van der Wiel, K., Bloomfield, H.C., Lee, R.W., Stoop, L.P., Blackport, R., Screen, J.A., Selten, F.M.: The influence of weather regimes on european renewable energy production and demand. *Environmental Research Letters* **14**(9), 094010 (2019) 1197
1198
1199
1200
1201

[59] Bevacqua, E., Zappa, G., Lehner, F., Zscheischler, J.: Precipitation trends determine future occurrences of compound hot–dry events. *Nature Climate Change* **12**(4), 350–355 (2022) 1202
1203
1204

[60] Bevacqua, E., Suarez-Gutierrez, L., Jézéquel, A., Lehner, F., Vrac, M., Yiou, P., Zscheischler, J.: Advancing research on compound weather and climate events via large ensemble model simulations. *Nature Communications* **14**(1), 2145 (2023) 1205
1206
1207
1208
1209

[61] WECC: Western Assessment of Resource Adequacy (2022). <https://www.wecc.org/Reliability/2022%20Western%20Assessment%20of%20Resource%20Adequacy.pdf> 1210
1211
1212
1213

[62] Rodgers, K.B., Lee, S.-S., Rosenbloom, N., Timmermann, A., Danabasoglu, G., Deser, C., Edwards, J., Kim, J.-E., Simpson, I.R., Stein, K., *et al.*: Ubiquity of human-induced changes in climate variability. *Earth System Dynamics* **12**(4), 1393–1411 (2021) 1214
1215
1216
1217
1218

[63] Craig, M.T., Jaramillo, P., Hodge, B.-M.: Carbon dioxide emissions effects of grid-scale electricity storage in a decarbonizing power system. *Environmental Research Letters* **13**(1), 014004 (2018) 1219
1220
1221
1222

[64] Jones, A.D., Rastogi, D., Vahmani, P., Stansfield, A., Reed, K., Ullrich, P., Rice, J.S.: Im3/hyperfacets thermodynamic global warming (tgw) simulation datasets. Technical report, MultiSector Dynamics-Living, Intuitive, Value-adding, Environment (2022) 1223
1224
1225
1226
1227

[65] GAMS: General algebraic modeling system (2024) 1228

[66] IBM: IBM ILOG CPLEX optimizer (2024) 1229
1230

[67] McKinnon, K.A., Simpson, I.R.: How unexpected was the 2021 pacific northwest heatwave? *Geophysical Research Letters* **49**(18), 2022–100380 (2022) 1231
1232
1233
1234

[68] Hart, W.E., Laird, C.D., Watson, J.-P., Woodruff, D.L., Hackebeil, G.A., Nicholson, B.L., Sirola, J.D., *et al.*: Pyomo-optimization Modeling in Python vol. 67. Springer, ??? (2017) 1235
1236
1237
1238

[69] GNU: GNU Linear Programming Kit (2020) 1239
1240

[70] Ruggles, T.H., Caldeira, K.: Wind and solar generation may reduce the 1241
1242

1243 inter-annual variability of peak residual load in certain electricity systems.
1244 Applied Energy **305**, 117773 (2022)

1245

1246 [71] Buster, G., Benton, B., Glaws, A., King, R.: sup3r (super resolution
1247 for renewable resource data)[swr-22-65]. Technical report, National
1248 Renewable Energy Laboratory (NREL), Golden, CO (United States)
1249 (2022)

1250

1251 [72] Losada Carreño, I., Craig, M.T., Rossol, M., Ashfaq, M., Batibeniz, F.,
1252 Haupt, S.E., Draxl, C., Hodge, B.-M., Brancucci, C.: Potential impacts of
1253 climate change on wind and solar electricity generation in texas. Climatic
1254 Change **163**, 745–766 (2020)

1255

1256 [73] Maraun, D.: Bias correcting climate change simulations - a critical review.
1257 Current Climate Change Reports **2**, 211–220 (2016)

1258

1259 [74] Hersbach, H., Bell, B., Berrisford, P., Biavati, G., Horányi, A.,
1260 Muñoz Sabater, J., Nicolas, J., Peubey, C., Radu, R., Rozum, I., et al.:
1261 Era5 hourly data on single levels from 1979 to present. Copernicus Climate
1262 Change Service (C3S) Climate Data Store (CDS) **10** (2018)

1263

1264 [75] Turner, S.W., Voisin, N., Nelson, K.D., Tidwell, V.C.: Drought impacts
1265 on hydroelectric power generation in the western united states. Technical
1266 report, Pacific Northwest National Lab.(PNNL), Richland, WA (United
1267 States) (2022)

1268

1269 [76] Turner, S.W., Voisin, N., Nelson, K.: Revised monthly energy genera-
1270 tion estimates for 1,500 hydroelectric power plants in the united states.
1271 Scientific Data **9**(1), 675 (2022)

1272

1273 [77] Murphy, S., Sowell, F., Apt, J.: A time-dependent model of generator fail-
1274 ures and recoveries captures correlated events and quantifies temperature
1275 dependence. Applied Energy **253**, 113513 (2019)

1276

1277 [78] Craig, M.T., Jaramillo, P., Hodge, B.-M., Nijssen, B., Brancucci, C.: Com-
1278 pounding climate change impacts during high stress periods for a high
1279 wind and solar power system in texas. Environmental Research Letters
15(2), 024002 (2020)

1280

1281 [79] US energy storage monitor - Q1 2024 and 2023 year in review exec-
1282 utive summary. Technical report, Wood Mackenzie Power & Renew-
1283 ables and American Clean Power (Mar 2024). [https://go.woodmac.com/](https://go.woodmac.com/usesm2024q1es)
1284 usesm2024q1es Accessed 2024-06-12

1285

1286 [80] Antonio, K., Mey, A.: U.S. battery storage capacity expected to nearly
1287 double in 2024 - U.S. Energy Information Administration (EIA) (2024).

1288

<https://www.eia.gov/todayinenergy/detail.php?id=61202> Accessed 2024-06-12 1289
1290
1291

[81] Brown, P.R., Botterud, A.: The value of inter-regional coordination and transmission in decarbonizing the us electricity system. *Joule* **5**(1), 115–134 (2021) 1292
1293
1294

[82] Yalew, S.G., van Vliet, M.T., Gernaat, D.E., Ludwig, F., Miara, A., Park, C., Byers, E., De Cian, E., Piontek, F., Iyer, G., *et al.*: Impacts of climate change on energy systems in global and regional scenarios. *Nature Energy* **5**(10), 794–802 (2020) 1295
1296
1297
1298
1299

[83] Hilbers, A.P., Brayshaw, D.J., Gandy, A.: Importance subsampling: improving power system planning under climate-based uncertainty. *Applied Energy* **251**, 113114 (2019) 1300
1301
1302
1303

[84] Waskom, M.L.: seaborn: statistical data visualization. *Journal of Open Source Software* **6**(60), 3021 (2021). <https://doi.org/10.21105/joss.03021> 1304
1305
1306

[85] Jerez, S., Tobin, I., Vautard, R., Montávez, J.P., López-Romero, J.M., Thais, F., Bartok, B., Christensen, O.B., Colette, A., Déqué, M., Nikulin, G., Kotlarski, S., Van Meijgaard, E., Teichmann, C., Wild, M.: The impact of climate change on photovoltaic power generation in Europe. *Nat. Commun.* **6** (2015). <https://doi.org/10.1038/ncomms10014> 1307
1308
1309
1310
1311
1312

[86] Blair, N., Diorio, N., Freeman, J., Gilman, P., Janzou, S., Neises, T., Wagner, M.: System advisor model (sam) general description (version 2017.9.5). National Renewable Energy Laboratory Technical Report (2018) 1313
1314
1315
1316

[87] TamizhMani, G., Ji, L., Tang, Y., Petacci, L., Osterwald, C.: Photovoltaic module thermal/wind performance: long-term monitoring and model development for energy rating. In: NCPV and Solar Program Review Meeting Proceedings, 24-26 March 2003, Denver, Colorado (CD-ROM) (2003). National Renewable Energy Lab., Golden, CO.(US) 1317
1318
1319
1320
1321

[88] Ruggles, T.H., Farnham, D.J., Tong, D., Caldeira, K.: Developing reliable hourly electricity demand data through screening and imputation. *Scientific data* **7**(1), 1–14 (2020) 1322
1323
1324
1325

[89] EIA: Form EIA-860 Annual Electric Generator Report. <https://www.eia.gov/electricity/data/eia860> 1326
1327
1328

[90] Akar, S., Beiter, P., Cole, W., Feldman, D., Kurup, P., Lantz, E., Margolis, R., Oladosu, D., Stehly, T., Rhodes, G., *et al.*: 2020 annual technology baseline (atb) cost and performance data for electricity generation technologies. Technical report, National Renewable Energy Laboratory-Data (NREL-DATA), Golden, CO (United States) (2020) 1329
1330
1331
1332
1333
1334

1335 [91] Wu, G.C., Jones, R.A., Leslie, E., Williams, J.H., Pascale, A., Brand,
1336 E., Parker, S.S., Cohen, B.S., Fargione, J.E., Souder, J., *et al.*: Minimiz-
1337 ing habitat conflicts in meeting net-zero energy targets in the western
1338 united states. *Proceedings of the National Academy of Sciences* **120**(4),
1339 2204098120 (2023)

1340

1341 [92] Miller, L.M., Keith, D.W.: Observation-based solar and wind power capac-
1342 ity factors and power densities. *Environmental Research Letters* **13**(10),
1343 104008 (2018)

1344

1345 [93] EPA: U.S. Environmental Protection Agency 2023 National Electric
1346 Energy Data System (Version 6.0). Online (2023). <https://www.epa.gov/airmarkets/national-electric-energy-data-system-needs-v6>

1347

1348 [94] EIA: Carbon Dioxide Emissions Coefficients. Online (2020). https://www.eia.gov/environment/emissions/co2_vol_mass.php

1349

1350

1351 [95] Brown, M., Cole, W., Eurek, K., Becker, J., Bielen, D., Chernyakhovskiy,
1352 I., Cohen, S., Frazier, A., Gagnon, P., Gates, N., *et al.*: Regional energy
1353 deployment system (reeds) model documentation: Version 2019. Technical
1354 report, National Renewable Energy Lab.(NREL), Golden, CO (United
1355 States) (2020)

1356

1357 [96] Jenkins, J.D., Sepulveda, N.A.: Enhanced decision support for a changing
1358 electricity landscape: the genx configurable electricity resource capacity
1359 expansion model (2017)

1360

1361 [97] NREL: ReEDS OpenAccess. github (2020). https://github.com/atpham88/ReEDS_OpenAccess

1362

1363

1364

1365

1366

1367

1368

1369

1370

1371

1372

1373

1374

1375

1376

1377

1378

1379

1380